Food Chemistry 306 (2020) 125619

Contents lists available at ScienceDirect

Food Chemistry

journal homepage: www.elsevier.com/locate/foodchem

Interfacial and colloidal characterization of oil-in-water emulsions stabilized by interface-tunable solid lipid nanoparticles

Honggu Lim[a,1], Myeongsu Jo[b,1], Choongjin Ban[e,f,*], Young Jin Choi[b,c,d,*]

[a] LG Electronics, 51 Gasan Digital 1 ro, Geumcheongu, Seoul 08592, Republic of Korea
[b] Department of Agricultural Biotechnology, Seoul National University, 1 Gwanakro, Gwanakgu, Seoul 08826, Republic of Korea
[c] Research Institute of Agriculture and Life Sciences, Seoul National University, 1 Gwanakro, Gwanakgu, Seoul 08826, Republic of Korea
[d] Center for Food and Bioconvergence, Seoul National University, 1 Gwanakro, Gwanakgu, Seoul 08826, Republic of Korea
[e] Institute of Biomolecule Control, Sungkyunkwan University, Seoburo 2066, Suwon, Gyeonggi 16419, Republic of Korea
[f] Biomedical Institute for Convergence, Sungkyunkwan University, Seoburo 2066, Suwon, Gyeonggi 16419, Republic of Korea

ARTICLE INFO

Keywords:
Colloidal stability
Contact angle
Interfacial characteristics
Pickering emulsion
Solid lipid nanoparticle
Surface load

ABSTRACT

We evaluated the correlation between the interfacial characteristics of solid lipid nanoparticles (SLNs) and the interfacial/colloidal stability of SLN-stabilized emulsions. Herein, the interfacial properties of SLNs, particularly the surface load (Γ_s) of emulsifiers, were tuned by controlling the type/concentration of emulsifier used to prepare the SLNs. Increasing the Γ_s decreased the contact angle at the oil–water interface, which enhanced the displacement free energy of the SLNs at the interface. Moreover, the Γ_s of emulsifiers bound to the surface of SLNs covering oil droplets was linearly correlated with the SLN-own Γ_s. The size/ζ-potential of emulsions stabilized by SLNs covered by the highest concentration of emulsifiers was unchanged for 1 month, indicating good emulsion stability. The interfacial/colloidal stability of SLN-stabilized emulsions was thus enhanced by increasing the emulsifier concentration used to produce the SLNs. This study provides baseline data for developing SLN-stabilized emulsions for the food, cosmetic, and pharmaceutical industries.

1. Introduction

Oil-in-water (O/W) emulsions are widely applied in the food, cosmetic, and pharmaceutical industries. These conventional systems are interfacially stabilized using small amphiphilic molecules such as phospholipids, surfactants, proteins, and other emulsifiers. However, they readily destabilize over time through aggregation and coalescence of the emulsion droplets, due to their thermodynamic instability (D.J. McClements, 2012). Conventional emulsions are inherently unstable with respect to changes in pH, ions, and temperature (Guzey & McClements, 2006). Pickering emulsions have been developed to overcome these limitations (Berton-Carabin & Schroën, 2015). Solid particles present at the interface of Pickering emulsions improve interfacial stability against coalescence (Dickinson, 2010; Pichot, Spyropoulos, & Norton, 2009), shear (Kotula & Anna, 2012; Thompson, Williams, & Armes, 2015), and freezing/thawing (Marefati, Rayner, Timgren, Dejmek, & Sjöö, 2013; Zhu, Zhang, Lin, & Tang, 2017). Many biocompatible and biodegradable solid particles have been evaluated as Pickering stabilizers, including starches (Sjöö, Emek, Hall, Rayner, & Wahlgren, 2015), chitin particles (Tzoumaki, Moschakis, Kiosseoglou, & Biliaderis, 2011), protein particles (Zhu et al., 2017), and lipid crystals (Frasch-Melnik, Spyropoulos, & Norton, 2010) or particles (Gupta & Rousseau, 2012).

Solid lipid nanoparticles (SLNs) are O/W emulsion-like systems comprising high-melting-point lipids. The physicochemical and interfacial properties of SLNs are easily tuned by changing the type and concentration of emulsifiers used in their preparation (Ban, Jo, Lim, & Choi, 2018). Several studies concerning O/W Pickering emulsions stabilized with SLNs have been reported (Gupta & Rousseau, 2012; Milsmann, Oehlke, Greiner, & Steffen-Heins, 2018; Milsmann, Oehlke, Schrader, Greiner, & Steffen-Heins, 2018; Pawlik, Kurukji, Norton, & Spyropoulos, 2016; Schröder, Sprakel, Schroën, & Berton-Carabin, 2017; Schröder, Sprakel, Schroën, Spaen, & Berton-Carabin, 2018; Zafeiri, Smith, Norton, & Spyropoulos, 2017). However, these studies did not investigate the correlation between SLN interfacial properties and the stability of SLN-stabilized Pickering emulsions. Especially, the

* Corresponding authors at: Institute of Biomolecule Control, Sungkyunkwan University, Seoburo 2066, Suwon, Gyeonggi 16419, Republic of Korea (C. Ban). Department of Agricultural Biotechnology, Seoul National University, 1 Gwanakro, Gwanakgu, Seoul 08826, Republic of Korea (Y.J. Choi).
E-mail addresses: pahncj@skku.edu (C. Ban), choiyj@snu.ac.kr (Y.J. Choi).
[1] These authors contributed equally to this work.

https://doi.org/10.1016/j.foodchem.2019.125619
Received 13 April 2019; Received in revised form 25 September 2019; Accepted 29 September 2019
Available online 03 October 2019
0308-8146/

amount of emulsifiers covering the SLNs (surface load, Γ_s) is a critical factor that determines the level of lipophilicity or hydrophilicity of the SLNs. The contact angle (θ) at the oil–water interface greatly influences the interfacial and colloidal stability of SLN-stabilized emulsions (Linke & Drusch, 2018). However, existing data on the interfacial behavior of SLNs are insufficient for assessing the correlation between Γ_s and θ.

In this study, SLNs were used to stabilize interface of the emulsion droplets. The physicochemical and interfacial characteristics of the SLNs were modulated by changing the type and concentration of PEGylated emulsifiers. The correlation between the Γ_s and θ of SLNs for impurity-free emulsifiers was determined using the gel-trapping technique, which simulates an oil–water interface, and atomic force microscopy (AFM) (Jo, Ban, Goh, & Choi, 2018). Moreover, the weight of emulsifier bound to the surface of the SLNs covering a unit surface of an emulsion droplet was quantified and defined as the bound Γ_s. The correlation between SLN–own Γ_s and the bound Γ_s was determined. Finally, the colloidal stability of the emulsions as a function of droplet size and surface charge was evaluated during storage for a month.

2. Materials and methods

2.1. Chemicals

Tristearin (Dynasan 118) was provided by IOI Oleochemicals GmbH (Hamburg, Germany). Polyoxyethylenesorbitan monostearate (Tween® 60 [T60]; molecular weight [MW], 1312 g mol^{-1}; hydrophilic–lipophilic balance [HLB], 14.9), polyoxyethylene (20) stearyl ether (Brij® S20 [B20]; MW, 1152 g mol^{-1}; HLB, 15), and polyoxyethylene (100) stearyl ether (Brij® S100 [B100]; MW, 4,670 g mol^{-1}; HLB, 18) were purchased from Sigma-Aldrich Co. (St. Louis, MO). Canola oil was obtained from CJ Cheiljedang Co. (Seoul, South Korea). All other chemicals were of analytical-reagent grade.

2.2. Fabrication of SLNs

The SLNs were prepared using a modified O/W emulsion technique reported previously (Ban et al., 2018). First, the lipid (2.5 wt%) and aqueous (97.5 wt%) phases were heated to 80 °C and mixed. The aqueous phase was prepared by dissolving the surfactants in 0.02 wt% sodium azide solution in double-deionized water (DDW) with stirring for 1 h (concentrations of surfactants in the aqueous phase: T60 and B20, 10–24 mmol kg^{-1}; B100, 3–8 mmol kg^{-1}). After mixing the lipid and aqueous phases, the droplet size was reduced via sonication (VCX 750; Sonics & Materials Inc., Newtown, CT) for 14 min at 60% amplitude (duty cycle of 1 s, 80 °C). Next, the SLN dispersion was cooled overnight in an ice bath and stored at 4 °C until it was used in subsequent experiments.

2.3. Dialysis of SLNs

Stabilization of the interface of emulsion droplets by unbound emulsifiers on the surface of the SLNs was excluded as follows. Any unbound emulsifier was removed from an SLN dispersion using dialysis membranes with a 1000-kDa MW cut-off (MWCO) (Spectra/PorBiotech, 131492; Spectrum Laboratories, Rancho Dominguez, CA). The bags were immersed in DDW for 12 h before use. Next, the bags were filled with 30 g of SLNs, tightly sealed, and suspended for 3 weeks in 5 L of DDW at 25 °C. After dialysis, the SLNs were removed from the bags and diluted to 75 g with DDW. The final concentration of tristearin in the diluted SLN dispersions was 1 wt%.

2.4. Preparation of O/W emulsions stabilized by SLNs

The O/W Pickering emulsions were prepared as follows. A mixture of canola oil (8.3 g, 10.0 wt%) and the diluted SLN dispersion (75 g, 0.9 wt% based on the weight of tristearin) was homogenized using a high-speed blender (Ultra-Turrax T25D; Ika Werke GmbH & Co., Staufen, Germany) at 7000 rpm for 2 min. The droplet size of the coarse emulsion was further reduced using a probe-type sonicator (VCX 750; Sonics & Materials Inc.) for 4 min at 60% amplitude with 1 s on/3 s off cycles. The temperature was maintained at 2 °C to prevent heat-induced melting of the particles. The prepared emulsions were stored at 4 °C until they were used in subsequent experiments.

2.5. Measurement of particle size and ζ-potential

The z-average particle size and ζ-potential of SLNs dialyzed and then diluted 200-fold with DDW were measured via dynamic laser scattering (DLS) using a Nano ZS90 instrument (Malvern Instruments Ltd., Malvern, UK) operating at a 173° angle and equipped with a helium-neon laser (λ = 633 nm). Zeta-potential measurements were based on the Smoluchowski equation at 25 °C and an electric field strength of 20 V cm^{-1}. The pH-dependent colloidal stability of SLNs diluted 50-fold with phosphate-buffered saline (PBS) was assessed as follows. The dilute solution was adjusted to the predetermined pH (3–7) using 1 M NaOH or 1 M HCl while monitoring with a pH meter (Professional Meter PP-15; Sartorius AG, Göttingen, Germany). The z-average particle size and ζ-potential of the SLNs were then measured using the Nano ZS90 instrument. Additionally, the De Brouckere ($D_{4,3}$) and Sauter ($D_{3,2}$) mean diameters of the dialyzed SLNs were measured via laser diffraction (LD) using a Mastersizer 2000 instrument (Malvern Instruments Ltd.) equipped with a Hydro 2000S dispersion cell. A refractive index of 1.49 was used for tristearin. The mean droplet sizes ($D_{4,3}$ and $D_{3,2}$) of the O/W Pickering emulsions were measured using the Mastersizer 2000 instrument equipped with a dispersion cell to evaluate stability during storage for 1 month. A refractive index of 1.472 was used for canola oil.

2.6. Differential scanning calorimetry

The polymorphism of the SLNs was determined using a differential scanning calorimeter (DSC, Discovery Series DSC 250; TA Instruments, Zellik, Belgium). Each sample (~5 mg) was placed in a hermetic aluminum pan, which was sealed and equilibrated at 25 °C overnight prior to measurement. An empty pan was used as a reference. The DSC scan began at a temperature of 25 °C, which increased by 3 °C min^{-1} to 95 °C. Thermograms were obtained using TRIOS software (TA Instruments).

2.7. Transmission electron microscopy

The micro-morphology of the SLNs was observed using an energy-filtering transmission electron microscope (TEM; LIBRA 120; Carl Zeiss, Oberkochen, Germany) operating at 120 kV. Ten microliters of SLNs diluted 25-fold with DDW were placed on a film-coated copper grid and negatively stained with a 1% (w/v) aqueous solution of phosphotungstic acid for 30 s. Next, the overflow solution was wiped off and the grid was dried in a desiccator for 1 h at 25 °C before observation.

2.8. Contact angle determination

The contact angle of SLNs at the oil–water interface was determined using a slightly modified gel-trapping technique (Jo et al., 2018). Canola oil was used as the oil phase and 1.5% w/v gellan (gel-forming agent) in 0.5 mM $CaCl_2$ as the water phase. Polydimethylsiloxane (PDMS) and Sylgard 184 elastomer (Dow Corning, Midland, MI) were used as curing agents at a 10:1 ratio, and SLNs were used as spreading particles. First, the gellan solution was heated to 121 °C for 15 min to dissolve and hydrate the gellan, and 20 mL of the solution was transferred to a Petri dish. Next, 20 mL of canola oil was placed on the gellan solution and gently shaken to create a flat oil–water interface. Subsequently, 0.3 mL of the dialyzed SLNs (tristearin, 0.5 wt%) was injected

at the oil–water interface (at ~42 °C). The dish was shaken sufficiently to distribute the SLNs at the interface as a monolayer and rapidly cooled to 25 °C for the gel to set. One hour later, the oil phase was carefully removed and immediately replaced with PDMS. After curing the PDMS at 25 °C for 48 h, the layer of PDMS entrapping the interfacial SLNs was peeled from the aqueous gel and washed with DDW.

The surface morphology of the PDMS layer entrapping the SLNs (PDMS-SLN) was observed using AFM to determine the θ of the SLNs at the oil–water interface. The observation was performed using an AC-mode Cypher S AFM (Asylum Research, Santa Barbara, CA) equipped with a standard non-contact probe (PR-T300; Probes, Seongnam, South Korea). For the θ determination using this technique, the tip of the AFM cantilever was used to determine the height (h) of the SLN portions protruding from the interface between the water and PDMS layers (a substitute for canola oil). However, particle diameters were not estimated from the AFM images due to convolution effects with the tip. Instead, one-half of the $D_{4,3}$ value (radius, R) of the SLNs was used to calculate the θ using the equation $\theta = \arccos(h/R - 1)$, with the assumption that the SLNs had a spherical shape.

2.9. Determination of the emulsifier surface load

The weight of emulsifier covering (bound to) a unit surface of tristearin matrices in the SLNs (Γ_s) was calculated as follows:

$$\Gamma_s = C_b D_{SLN}/6\Phi_{SLN}$$

where C_b is the concentration of emulsifier bound to the surface of the SLNs, D_{SLN} is the $D_{3,2}$ of the SLNs, and Φ_{SLN} is the volume fraction of tristearin (*i.e.*, ~0.029). The method for determining C_b was modified from that reported previously by our group (Ban et al., 2018). The C_b of the SLNs was calculated by subtracting the unbound emulsifier concentration from the total emulsifier concentration. Briefly, non-dialyzed T60-, B20-, and B100-prepared SLN dispersions were first diluted 20-, 20-, and 500-fold with DDW, respectively. The diluted dispersions were passed through polyvinylidene difluoride membrane syringe filters (0.45 μm, 25 mm GD/X; Whatman Ltd., Loughborough, UK) to remove aggregates, and centrifuged in Vivaspin® 6 centrifugal concentrators (MWCO 1000 kDa; Sartorius AG, Göttingen, Germany) using a Universal 320R centrifuge (Hettich, Tuttlingen, Germany) (2,370 relative centrifugal force [RCF], 40 min, 20 °C). Next, 2 mL of filtrates in microtubes were completely dried in an oven at 65 °C for 48 h, cooled to ambient temperature, and combined with 0.5 mL of ammonium cobaltothiocyanate solution and 1.0 mL of dichloromethane. The ammonium cobaltothiocyanate solution was prepared by dissolving 3 g of cobalt nitrate hexahydrate and 18 g of ammonium thiocyanate in 100 mL of DDW. The microtubes were vortexed for 10 s and centrifuged for 10 min at 10,400 RCF and 25 °C (5427R; Eppendorf AG, Hamburg, Germany). After centrifugation, the dichloromethane layer was transferred to a micro quartz cell and its absorbance at 625 nm was measured using a spectrophotometer (Pharmaspec UV-1700; Shimadzu Corp., Kyoto, Japan). The emulsifier concentration in the samples was calculated from standard curves over the ranges 50–1000, 50–1000, and 1–10 μmol kg^{-1} for T60, B20, and B100 (R^2 = 0.9996, 0.9997, and 0.9964), respectively.

The Γ_s values of the Pickering emulsions were calculated separately for the emulsifiers bound to the SLNs and the unbound emulsifiers covering the droplets. The bound Γ_s was calculated as follows:

$$\Gamma_s \text{ (bound)} = C_B D_{PE}/6\Phi_{PE}$$

where C_B is the concentration of bound emulsifiers, D_{PE} is the $D_{3,2}$ particle size of the Pickering emulsions, and Φ_{PE} is the volume fraction of canola oil (~0.107). The C_B was estimated as $C_b/2.5$, because 30 g of SLNs were diluted to 75 g with DDW before Pickering emulsion preparation and we assumed that all bound emulsifiers remained on the surface of the SLNs during preparation of the Pickering emulsions. The unbound Γ_s was calculated using the following equation:

$$\Gamma_s \text{ (unbound)} = C_U D_{PE}/6\Phi_{PE}$$

where C_U is the concentration of unbound emulsifiers. C_U was determined using the same method as C_b, except that dialyzed SLN dispersions were used instead of non-dialyzed dispersions. Using the calculated values of C_B and C_U, the bound ratio was calculated as $C_B/(C_B + C_U)$.

2.10. Polarized light microscopy

Polarized light microscopy (PLM; Eclipse LV 100 ND; Nikon, Kyoto, Japan) was used to validate the coverage of SLNs on the surface of the oil droplets. Emulsions were produced using the hand-shaking method as described previously (Schröder et al., 2017). In a 15 mL tube, 0.5 g of canola oil and 4.5 g of the dialyzed SLN dispersion (tristearin, 1 wt%) were hand-shaken for 10 s and diluted 10-fold with DDW.

2.11. Statistical analyses

Data were averaged over at least three independent experiments or measurements. More than 20 AFM images were analyzed to determine the θ of the SLNs. The results are reported as averages and standard deviations. Correlation curves were plotted and fitted using the linear regression procedures in SigmaPlot 10.0 software for Windows (Systat Software, San Jose, CA).

3. Results and discussion

3.1. Physicochemical characteristics of SLNs

The predetermined emulsifier concentration ranges used to prepare SLNs were 10–24, 10–24, and 3–8 mmol kg^{-1} for T60, B20, and B100, respectively. These ranges were based on the non-gelling behavior of the prepared SLNs. Within these ranges, the fabricated SLNs had a unimodal particle size distribution according to both the DLS and LD methods, irrespective of sample dilution. The z-average particle size decreased (T60, 194 → 69 nm; B20, 205 → 126 nm; B100, 277 → 219 nm) with increasing emulsifier concentration (Fig. 1a); the $D_{4,3}$ values also decreased (T60, 163 → 126 nm; B20, 179 → 149 nm; B100, 324 → 202 nm) (Fig. 1c). These trends reflected the emulsifier's ability to function even as the surface tension increased during the size reduction process (Aveyard, Binks, & Clint, 2003). The discrepancy between the z-average and $D_{4,3}$ particle size is attributed to dilution of the samples for DLS or to the different ways of determining particle size using the two methods. TEM images of the SLNs (Fig. 2) revealed that they were almost spherical. The size of the SLNs in these images was in good agreement with their $D_{4,3}$ values.

The emulsifiers used in this study contain a hydrophilic polyethylene glycol (PEG) chain, and tristearin contains electrically negative fatty acid impurities (McClements & Xiao, 2012). For instance, the fatty acids possibly present at the tristearin–water interface of the SLNs as tristearin impurities have smaller hydrophilic portions (carboxylic acid) than T60, B20, and B100. Moreover, their lipophilic tails can penetrate deeper into the tristearin phase than T60, B20, and B100, because these fatty acids are more lipophilic than those of T60, B20, and B100. Therefore, the larger hydrophilic chains (PEG chains) of T60, B20, and B100 protruded toward the water phase from the interface and spatially covered the carboxylic acids of the fatty acids. When we prepared SLNs without emulsifiers, the ζ-potential value was −57.7 mV. This suggests that negatively charged tristearin impurities were present at the interface of the SLNs prepared using only tristearin. Also, T60, B20, and B100, as non-ionic surfactants, are electrically neutral.

In this respect, if the emulsifiers fully covered the surface of the SLNs, the surface charge of the SLNs would be zero due to electrical neutralization by the PEG molecules at the tristearin–water interface.

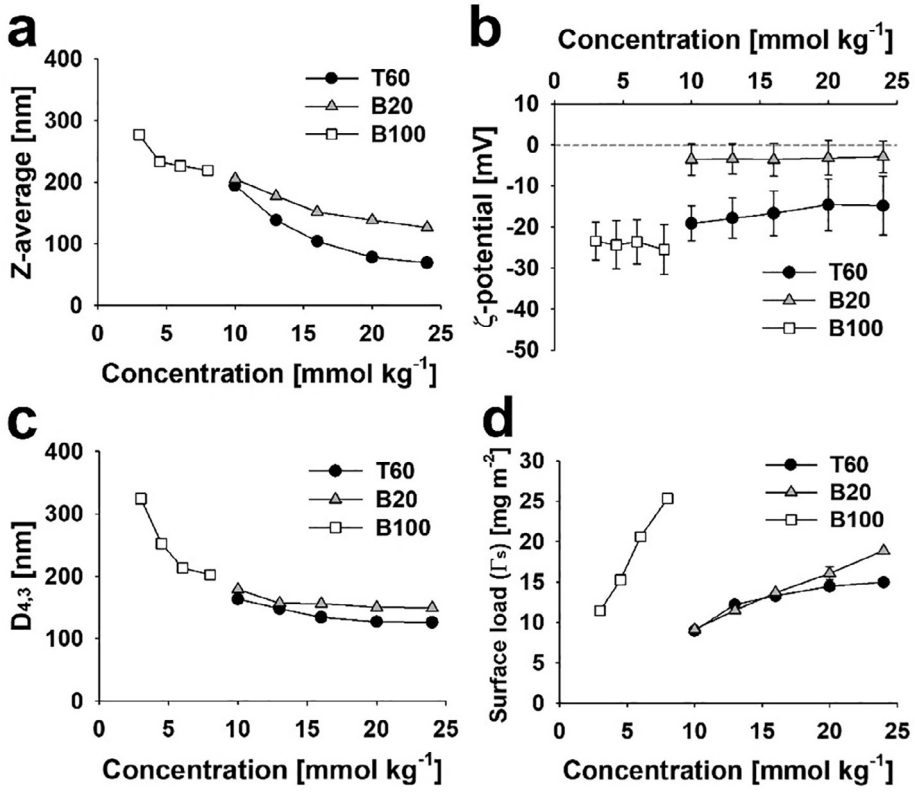

Fig. 1. (a) Z-average particle size, (b) ζ-potential, (c) De Brouckere mean diameter ($D_{4,3}$), and (d) surface load (Γ_s) of SLNs emulsified using Tween® 60 (T60), Brij® S20 (B20), and Brij® S100 (B100).

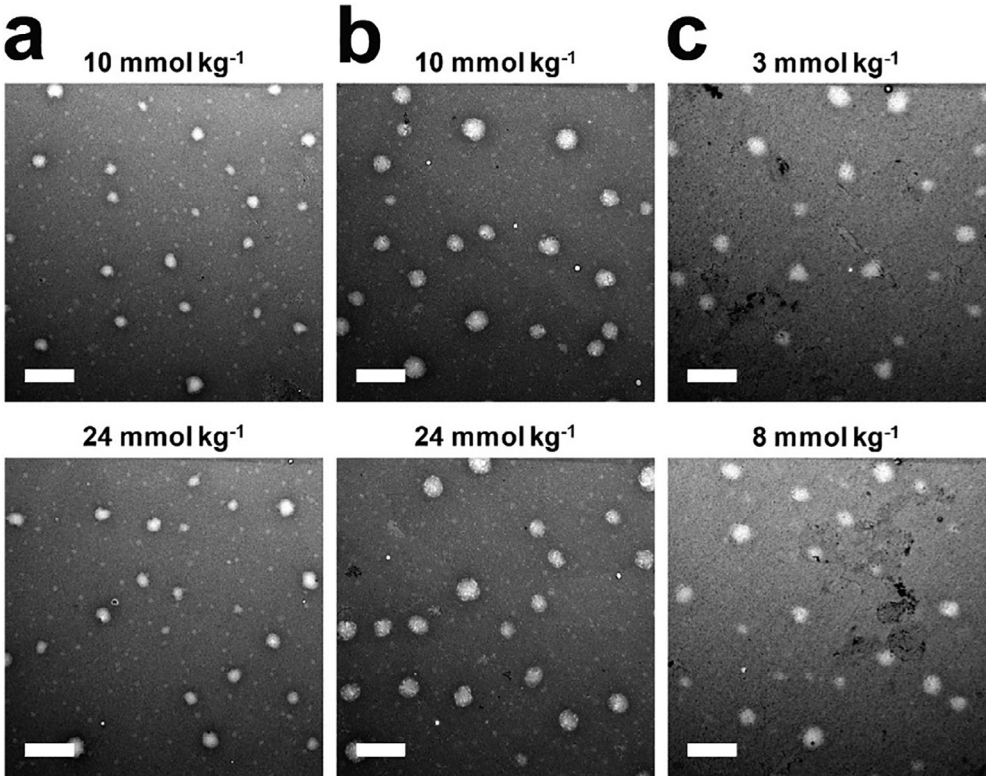

Fig. 2. Transmission electron micrographs of SLNs emulsified using (a) Tween® 60 (10 and 24 mmol kg^{-1}), (b) Brij® S20 (10 and 24 mmol kg^{-1}), and (c) Brij® S100 (3 and 8 mmol kg^{-1}) (bars, 1 μm).

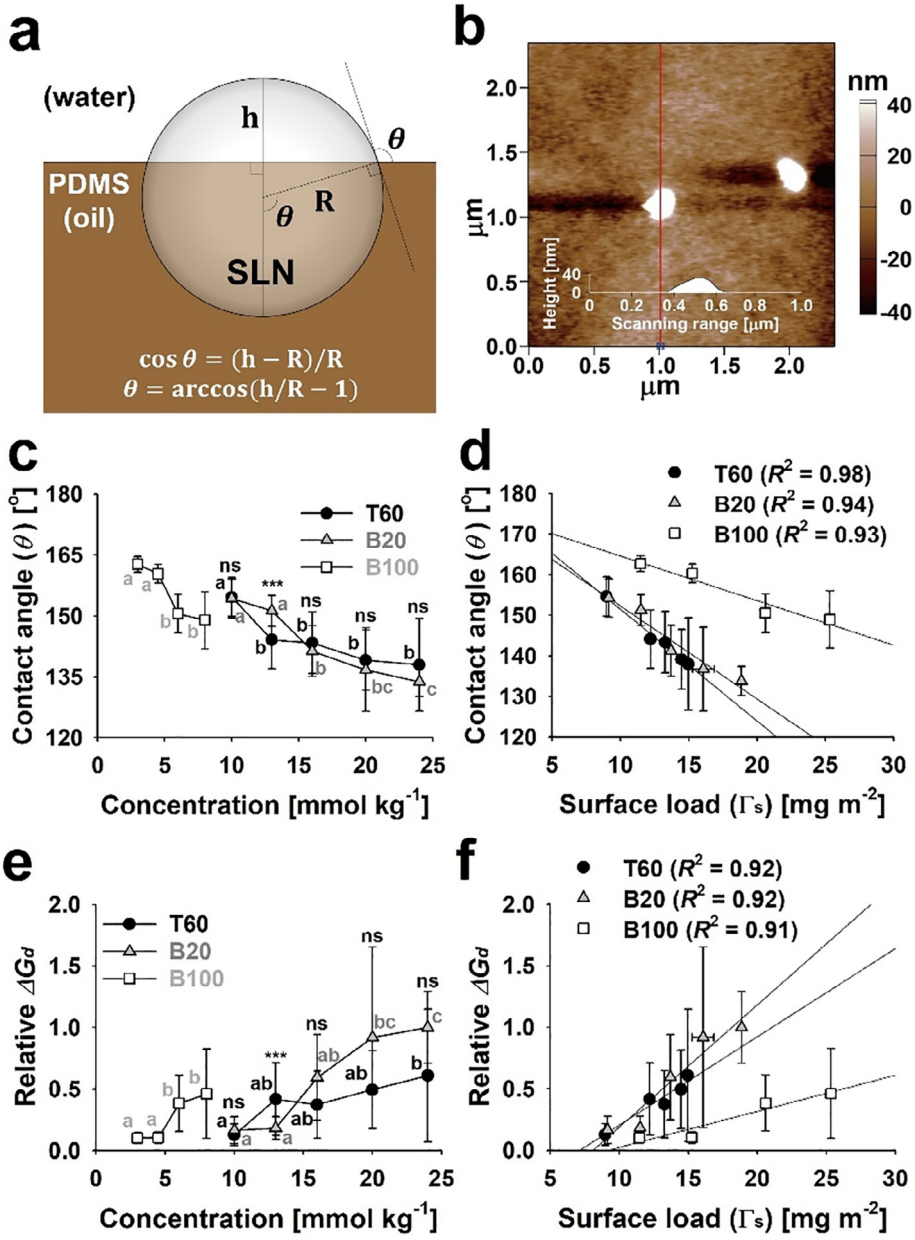

Fig. 3. (a) Schematic representation of the contact angle (θ) of SLNs embedded at the interface between the oil (polydimethylsiloxane [PDMS]) and water phases. (b) Representative atomic force micrograph and height profile of SLNs embedded at the interface, obtained using the gel-trapping technique. (c) Contact angle (θ) ($n \geq 20$) of SLNs emulsified using Tween® 60 (T60), Brij® S20 (B20), and Brij® S100 (B100). (d) Linear correlation curves of the contact angle (θ) as a function of the surface load (Γ_s). (e) Relative displacement free energy (ΔG_d) of the SLNs at the oil–water interface. (f) Linear correlation curves of relative ΔG_d as a function of Γ_s. Relative ΔG_d was defined as the ΔG_d of the specific SLNs divided by the ΔG_d of the SLN prepared using 24 mmol kg^{-1} of B20. Different letters (a–c) for each group (T60, B20, or B100) indicate significant differences based on Tukey's honestly significant difference test ($p < 0.05$); ns and *** indicate non-significant and significant differences between the T60 and B20 groups based on the Student's *t*-test ($p > 0.05$ and < 0.001, respectively).

However, Fig. 1b shows that the ζ-potential values of the SLNs were non-zero, suggesting incomplete surface coverage by the emulsifiers. The ζ-potential values of the T60-, B20-, and B100-emulsified SLNs were −19 to −15, approximately −3, and approximately −24 mV, respectively, indicating that B20 provided the greatest coverage. The Γ_s values of the T60-, B20-, and B100-emulsified SLNs increased (T60, $9 \rightarrow 15$ mg m^{-2}; B20, $9 \rightarrow 19$ mg m^{-2}; B100, $11 \rightarrow 25$ mg m^{-2}) with increasing emulsifier concentration (Fig. 1d). Considering both the ζ-potential and Γ_s values of the SLNs, B20 was the optimal emulsifier for masking the interfacial negative charge originating from tristearin impurities. The different charge-masking effectiveness of the emulsifiers might have resulted from differences in the spatial arrangement of the hydrophilic PEG chains (Ban et al., 2018) and/or depth of emulsifiers anchored or adhered to the interface (Salminen et al., 2014).

Fig. S1a shows that the z-average particle size of the SLNs prepared with emulsifiers at the lowest or highest concentration was unchanged over the pH range 3–7. This indicates pH-independent colloidal stability irrespective of the type or concentration of emulsifiers. By contrast, the ζ-potential of the SLNs changed with pH and was almost zero at pH 3 (Fig. S1b), indicating electrical neutralization of the impurities, such as fatty acids, in tristearin (Ban et al., 2018; Wellen, Lach & Allen, 2017). Nevertheless, the colloidal stability of the SLNs was maintained over the examined pH range (Fig. S1a). This indicates that the emulsifiers sufficiently covered the interface and successfully prevented flocculation and aggregation of the lipid particles, even though the emulsifiers were unable to completely mask the interfacial negative charge.

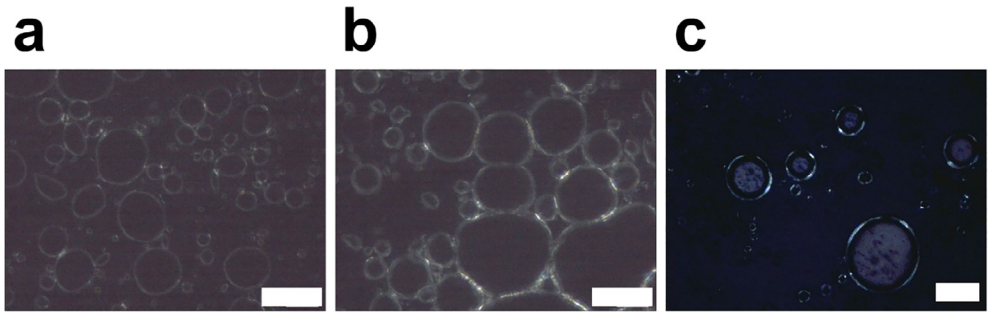

Fig. 4. Polarized light micrographs of emulsions stabilized using SLNs emulsified with (a) Tween® 60 (24 mmol kg^{-1}; bar, 40 μm), (b) Brij® S20 (24 mmol kg^{-1}; bar, 40 μm), and (c) Brij® S100 (8 mmol kg^{-1}; bar, 60 μm) via the hand-shaking method.

Therefore, colloidal destabilization of Pickering emulsions covered by these SLNs did not result from flocculation or aggregation of the SLNs at the interface. In other words, the SLNs provided good stearic hindrance as stabilizers at the O/W interface of Pickering emulsions.

The DSC thermograms of the SLNs displayed endothermic peaks that correspond to the melting of polymorphic tristearin crystals (Fig. S2). Peaks at ~53.0, ~62.5, and ~69.0 °C were observed for all SLNs; these can be attributed to the melting of crystalline α, β', and β polymorphs, respectively, present in the tristearin matrices of the SLNs (Da Silva, Bresson, & Rousseau, 2009). The melting transition (T_m) of the crystals in the emulsion droplets was typically split because of the location of the polymorph, *i.e.*, on the surface or in the core of the droplets (Gülseren & Coupland, 2008). This is because the droplet core was relatively pure, but the surface was impure due to the presence of the lipophilic tails of the surfactants. The splitting trend of the T_m transition is in accordance with the molecular similarity between the lipophilic tail and the lipid. The lipophilic tails of the emulsifiers used were saturated C18 chains. The split T_m transitions for α-tristearin crystals were observed at ~50.5, ~45.5, and ~47.0 °C for the SLNs emulsified by T60, B20, and B100, respectively (Table S1). Additionally, the surfactants present at the tristearin–water interface quantitatively influenced the polymorphism of the SLNs prepared with high-melting-point triacylglycerol (Zafeiri, Norton, Smith, Norton, & Spyropoulos, 2017). Notably, high-melting-point surfactants such as T60 promote the formation of the α polymorph compared to low-melting-point surfactants such as Tween® 80 (Helgason et al., 2009).

To summarize the thermal characteristics of the SLNs, the high-melting-point emulsifiers (T60, B20, and B100) quantitatively influenced the formation of α-form tristearin crystals, including split α-crystals (α*-form crystals). Therefore, the correlation between the SLN-surface coverage (Γ_s) of the emulsifiers and the α-crystal-occupied percentage of the formed crystals (α-crystallization index) was evaluated based on crystal melting enthalpy (Table S1). Hence, the α-crystallization index was calculated as:

$$100 \times (\Delta H_{\alpha^*} + \Delta H_{\alpha})/(\Delta H_{\alpha^*} + \Delta H_{\alpha} + \Delta H_{\beta'} + \Delta H_{\beta})$$

where ΔH_{α^*}, ΔH_{α}, $\Delta H_{\beta'}$, and ΔH_{β} are the melting enthalpies for the α*-, α-, β′-, and β-form tristearin crystals in the SLNs, respectively. The α-crystallization index and Γ_s were linearly correlated (Fig. S3). Consequently, the T60-, B20-, and B100-emulsified SLNs had good colloidal stability and Γ_s, which was controlled by emulsifier concentration, influenced the crystallinity of the lipid matrix.

3.2. Oil–water interfacial behavior of the SLNs

The free energy of displacement (ΔG_d) for a Pickering particle at the oil–water interface is as follows (Gupta & Rousseau, 2012):

$$\Delta G_d = \pi R^2 \gamma_{ow} (1 - |\cos\theta|)^2$$

where γ_{ow} is the interfacial tension. The θ value of a Pickering stabilizer is a critical determinant of the stability of a Pickering emulsion. We used the previously reported gel-trapping technique with PDMS and gellan to measure the θ of the SLNs at the oil–water interface (Paunov, 2003). For this measurement, the height (h) of the SLN portions protruding from the interface of the PDMS embedding the SLNs (Fig. 3a) was measured using the tip of a AFM cantilever (Fig. 3b). The θ value of the SLNs was calculated using the following equation:

$$\theta = \arccos(h/R - 1).$$

The θ value gradually decreased with increasing emulsifier concentration (Fig. 3c; 155 → 138°, 154 → 134°, and 163 → 149° for T60, B20, and B100, respectively). Larger values indicate the predominance of lipophilicity rather than hydrophilicity of the SLNs. Notably, Fig. 3d shows an excellent linear correlation ($R^2 > 0.93$) between the θ and Γ_s values of the SLNs. This indicates that the hydrophilicity of SLNs can be increased by increasing the emulsifier loading on their surface.

Narrowing of the obtuse angle θ by increasing Γ_s increased the ΔG_d of the SLNs, which improved the interfacial stability of SLN-stabilized emulsions. The experimental R and θ values, and a constant γ_{ow} value, were used to calculate the relative ΔG_d of the SLNs to assess their potential as Pickering stabilizers (Fig. 3e). The relative ΔG_d for a specific SLN was defined as its ΔG_d over the ΔG_d (*i.e.*, its maximum ΔG_d) prepared using 24 mmol kg^{-1} of B20. For all SLNs, relative ΔG_d increased with increasing emulsifier concentration, indicating improved interfacial stability of the SLNs at the oil–water interface of the Pickering emulsion droplets. Additionally, the good linear correlation between relative ΔG_d and Γ_s indicated direct proportionality (Fig. 3f). Therefore, increasing the Γ_s of the SLNs allowed them to stabilize the oil–water interface and thereby improved the colloidal stability of the SLN-stabilized emulsions.

3.3. Interfacial characteristics and colloidal stability of emulsions stabilized by SLNs

The oil–water interface of the SLN-stabilized emulsions was visualized using PLM. Fig. 4 shows white monolayers of tristearin crystals covering the droplets at the interface of the oil droplets. Most of the droplets were spherical, but some non-spherical droplets stabilized by T60- and B20-emulsified SLNs were also observed (Fig. 4a and b). This suggests that the T60- and B20-emulsified SLNs covering the interface interfered with each other due to hydrophobic networks, which prevented surface tension-driven relaxation of the droplets to a spherical shape (Schröder et al., 2017). Additionally, particle-mediated bridging between the droplets, known to occur in Pickering emulsions stabilized with largely hydrophilic particles (Dickinson, 2010), was observed in micrographs of emulsions prepared with T60- and B20-emulsified SLNs. By contrast, the droplets stabilized by B100-emulsified SLNs were spherical (Fig. 4c); this is attributed to steric repulsion among the SLNs due to their large Γ_s value. Also, no bridging was found in emulsions prepared with the B100-emulsified SLNs, which is attributed to their greater θ value (149°) compared to the other SLNs.

In the present study, the SLNs were dialyzed before use. This

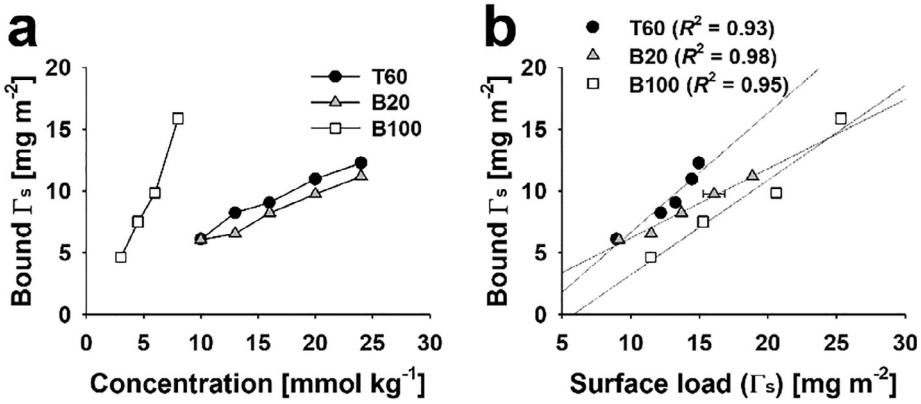

Fig. 5. (a) Weights of Tween® 60 (T60), Brij® S20 (B20), and Brij® S100 (B100) covering a unit surface of SLN-stabilized emulsion droplets and bound to the surface of SLNs (bound Γ_s). (b) Linear correlation curves of bound Γ_s as a function of the surface load (Γ_s) of the emulsifiers on SLNs.

ensured that the interface of the emulsions was stabilized only by the SLNs themselves and minimized coverage by free emulsifiers. Table S2 lists the calculated bound and unbound Γ_s values of the emulsifiers. Here, bound Γ_s refers to the weight of emulsifiers bound to the surface of the SLNs covering a unit surface of the emulsion droplets, and unbound Γ_s indicates the weight of free emulsifiers covering a unit surface of the droplets themselves. Over 95% of the emulsifiers used to produce the emulsions were bound to the surface of the SLNs (*i.e.*, the bound ratio in Table S2), suggesting that most of the interfacial area of the emulsions was stabilized not by free emulsifiers but rather by SLNs. The bound Γ_s values of the emulsions stabilized by T60-, B20-, and B100-SLNs increased to 12.27, 11.19, and 15.88 mg m^{-2}, respectively, with increasing emulsifier concentration (Fig. 5a). The excellent linear correlation between the bound Γ_s and Γ_s values of the SLNs indicates direct proportionality (Fig. 5b). Because the amount of SLNs used to make the emulsions was fixed based on the weight of tristearin (0.9 wt%), the interface of the emulsions became thicker as the bound Γ_s value increased. Therefore, increasing the concentration of emulsifiers used to prepare the SLNs enhanced the interfacial stability of the SLN-stabilized emulsions by enhancing steric hindrance at the interface.

Indeed, the emulsions prepared with SLNs emulsified using emulsifiers at the maximum concentrations (T60, 24 mmol kg^{-1}; B20, 24 mmol kg^{-1}; B100, 8 mmol kg^{-1}) were stable during storage for 1 month. The $D_{4,3}$ values of these emulsions changed only slightly during storage (T60, 3.3 → 3.3 μm; B20, 2.9 → 2.4 μm; B100, 3.3 → 2.9 μm) (Fig. 6a–c), and their volumetric size distributions were unchanged (Fig. 6g–i). However, the emulsions prepared with SLNs emulsified using emulsifiers at the minimum concentrations (T60, 10 mmol kg^{-1}; B20, 10 mmol kg^{-1}; B100, 3 mmol kg^{-1}) were unstable during storage. In this case, the $D_{4,3}$ value and the volumetric size distribution of the emulsions changed significantly (T60, 3.4 → 13.7 μm; B20, 3.3 → 1.4 μm; B100, 3.2 → 2.2 μm). A possible explanation for the decrease, rather than increase, in $D_{4,3}$ values after 1 month is the formation and creaming of droplets that were too large to be detected by the instrument (upper size limit of 600 μm). The destabilization of these emulsions cannot result from coagulation and flocculation among the emulsion droplets because the ζ-potentials of the emulsions were strongly negative and remained unchanged during storage (T60, −46 to −32 mV; B20, −40 to −32 mV; B100, −41 to −34 mV) (Fig. 6d–f). Moreover, SLN-mediated bridging between the droplets cannot explain the destabilization, because the emulsions stabilized by SLNs at the maximum concentrations of T60 and B20 had good storage stability despite the occurrence of the bridging phenomenon as observed using PLM (Fig. 4a and b).

Low-density networking among the SLNs in the film between closely approaching emulsion droplets likely explains the destabilization of the emulsions (Dickinson, 2010). Compared to the ζ-potential and Γ_s values of the SLNs (Fig. 1b and d), the emulsion produced with SLNs emulsified using 3 mmol kg^{-1} B100 (3 mmol kg^{-1} B100-SLN-emulsion; ζ-potential, −23 mV; Γ_s, 11.5 mg m^{-2}) displayed a more negative electrical potential and greater steric repulsion among particles than the 10 mmol kg^{-1} T60- and B20-SLN-emulsions (ζ-potential, −19 and −4 mV; Γ_s, 9.0 and 9.1 mg m^{-2}, respectively). After storage for 1 month, only slight creaming and size changes (Fig. 6c and i) were observed in the 3 mmol kg^{-1} B100-SLN-emulsion, compared to severe creaming and size changes in the 10 mmol kg^{-1} T60 and B20-SLN-emulsions (Fig. 6a, b, g, and h). These results suggest that the 3 mmol kg^{-1} B100-SLN-emulsion has greater storage stability than the 10 mmol kg^{-1} T60- and B20-SLN-emulsions, likely due to reduced low-density networking between the aggregated SLNs in the film.

In a comparison with conventional emulsions prepared with only T60, B20, or B100, the $D_{4,3}$ and ζ-potential values of the emulsifier-stabilized emulsions gradually increased and decreased during storage, respectively (Fig. S4a–f). Moreover, the volumetric size distributions of the emulsions shifted towards a larger size during storage (Fig. S4g–i). This destabilization is likely due to coalescence among the oil droplets, which might be caused by the rearrangement of the emulsifier at the oil–water interface. By contrast, the $D_{4,3}$ value, ζ-potential, and size distribution of the emulsions prepared with SLNs emulsified using 24 mmol kg^{-1} T60, 24 mmol kg^{-1} B20, or 8 mmol kg^{-1} B100 remained unchanged during storage (Fig. 6). This suggests that PEGylated emulsifier-stabilized SLNs had a larger ΔG_d value than PEGylated emulsifiers due to their large size, indicating problematic rearrangement at the interface. Thus, the SLN-stabilized emulsions are resistant to coalescence and are stable during storage.

Fig. 3e shows that the relative ΔG_d values of emulsions prepared with SLNs emulsified using emulsifiers at the minimum concentrations (T60, 0.13; B20, 0.16; B100, 0.10) were smaller than those of emulsions prepared with SLNs emulsified using emulsifiers at the maximum concentrations (T60, 0.61; B20, 1.00; B100, 0.46). All emulsions prepared with SLNs emulsified using emulsifiers at the minimum concentrations were unstable during storage. Thus, the low ΔG_d may also be a mechanism of destabilization. To summarize, the amount (Γ_s) of emulsifiers covering the unit surface of SLNs governs the colloidal stability of SLN-stabilized emulsions, because Γ_s proportionally influences both bound Γ_s and ΔG_d. Herein, Γ_s was controlled by modulating emulsifier concentration. Consequently, the interfacial and colloidal stability of the SLN-stabilized emulsions was enhanced by increasing the emulsifier concentration during the preparation of SLNs.

4. Conclusions

We examined the physicochemical and interfacial characteristics of SLNs prepared as Pickering stabilizers to understand the interfacial and colloidal stability of SLN-stabilized emulsions. The various SLNs were stable under aqueous conditions irrespective of the type or

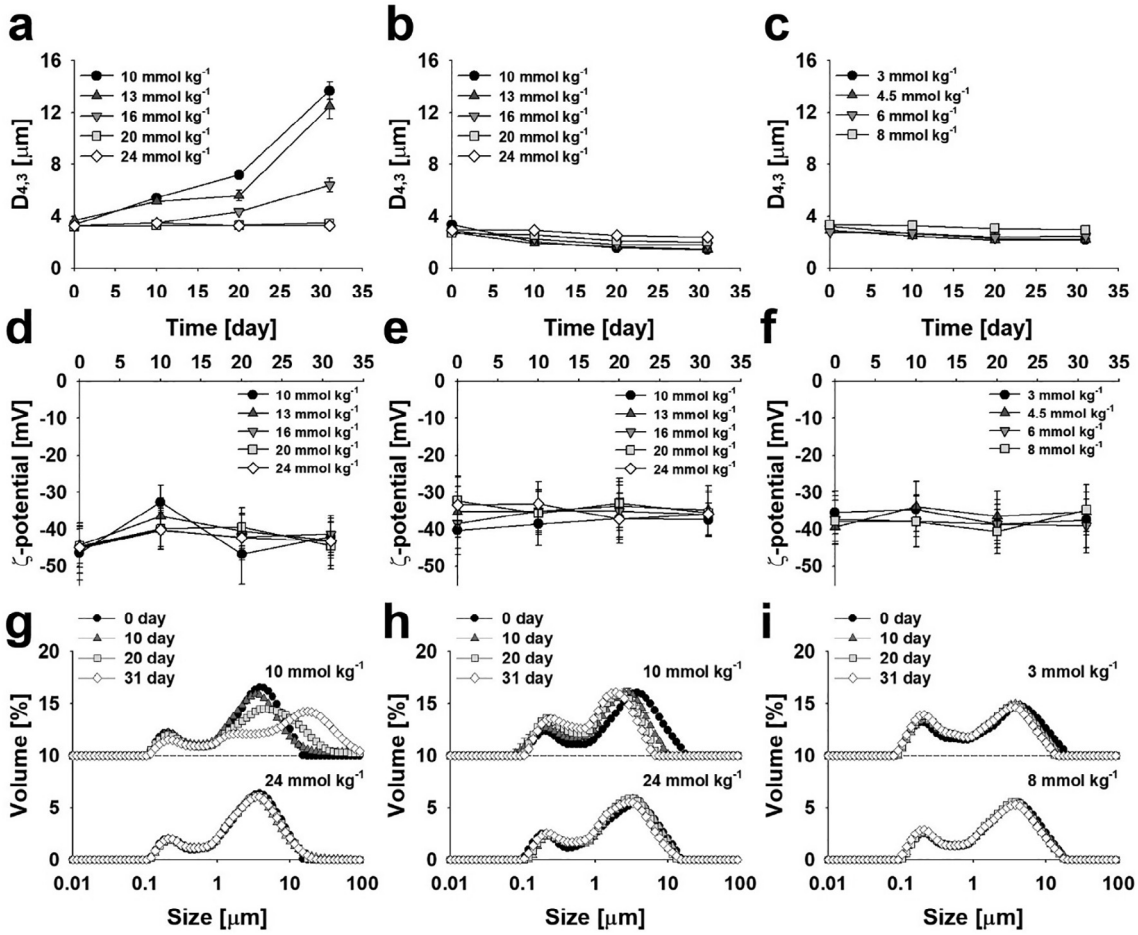

Fig. 6. Changes in (a–c) the De Brouckere mean diameter ($D_{4,3}$), (d–f) ζ-potential, and (g–i) volumetric size distribution of the emulsions stabilized by SLNs emulsified by (a, d, and g) Tween® 60, (b, e, and h) Brij® S20, and (c, f, and i) Brij® S100, during storage for 1 month.

concentration of emulsifiers. This was attributed to the steric hindrance effect of the PEGylated emulsifiers at the tristearin–water interface. Notably, increasing the Γ_s value of the SLNs, which was accomplished by increasing the emulsifier concentration, decreased θ and resulted in a proportional increase in ΔG_d. Additionally, increasing Γ_s also increased the bound Γ_s value of the emulsions. At the maximum concentration of emulsifiers for SLN preparation, the colloidal stability of the SLN-stabilized emulsions was enhanced due to the increased Γ_s value. These emulsions were colloidally stable during storage for 1 month. The interfacial and colloidal stability of SLN-stabilized emulsions can thus be improved by increasing the concentration of emulsifiers used to produce the SLNs. Our findings will facilitate the development of SLN-stabilized emulsions for the food, cosmetic, and pharmaceutical industries.

Declaration of Competing Interest

The authors declare that they have no known competing financial interests or personal relationships that could have appeared to influence the work reported in this paper.

Acknowledgment

This research was supported by the Basic Science Research Program through the National Research Foundation of Korea funded by the Ministry of Science, ICT, and Future Planning, South Korea (2016R1D1A1B03936106, 2017R1A6A1A03015642, and 2018R1D1A1B07050508).

Appendix A. Supplementary data

Supplementary data to this article can be found online at https://doi.org/10.1016/j.foodchem.2019.125619.

References

Aveyard, R., Binks, B. P., & Clint, J. H. (2003). Emulsions stabilised solely by colloidal particles. *Advances in Colloid and Interface Science, 100*, 503–546.
Ban, C., Jo, M., Lim, S., & Choi, Y. J. (2018). Control of the gastrointestinal digestion of solid lipid nanoparticles using PEGylated emulsifiers. *Food Chemistry, 239*, 442–452.
Berton-Carabin, C. C., & Schroën, K. (2015). Pickering emulsions for food applications: Background, trends, and challenges. *Annual Review of Food Science and Technology, 6*, 263–297.
Da Silva, E., Bresson, S., & Rousseau, D. (2009). Characterization of the three major polymorphic forms and liquid state of tristearin by Raman spectroscopy. *Chemistry and Physics of Lipids, 157*(2), 113–119.
Dickinson, E. (2010). Food emulsions and foams: Stabilization by particles. *Current Opinion in Colloid & Interface Science, 15*(1), 40–49.
Frasch-Melnik, S., Spyropoulos, F., & Norton, I. T. (2010). $W_1/O/W_2$ double emulsions stabilised by fat crystals – Formulation, stability and salt release. *Journal of Colloid and Interface Science, 350*(1), 178–185.
Gülseren, İ., & Coupland, J. N. (2008). Surface melting in alkane emulsion droplets as affected by surfactant type. *Journal of the American Oil Chemists' Society, 85*(5), 413–419.
Gupta, R., & Rousseau, D. (2012). Surface-active solid lipid nanoparticles as Pickering stabilizers for oil-in-water emulsions. *Food & Function, 3*(3), 302–311.
Guzey, D., & McClements, D. J. (2006). Formation, stability and properties of multilayer emulsions for application in the food industry. *Advances in Colloid and Interface Science, 128*, 227–248.
Helgason, T., Awad, T. S., Kristbergsson, K., Decker, E. A., McClements, D. J., & Weiss, J. (2009). Impact of surfactant properties on oxidative stability of β-carotene encapsulated within solid lipid nanoparticles. *Journal of Agricultural and Food Chemistry, 57*(17), 8033–8040.
Jo, M., Ban, C., Goh, K. K. T., & Choi, Y. J. (2018). Gastrointestinal digestion and stability

of submicron-sized emulsions stabilized using waxy maize starch crystals. *Food Hydrocolloids, 84*, 343–352.
Kotula, A. P., & Anna, S. L. (2012). Probing timescales for colloidal particle adsorption using slug bubbles in rectangular microchannels. *Soft Matter, 8*(41), 10759–10772.
Linke, C., & Drusch, S. (2018). Pickering emulsions in foods – Opportunities and limitations. *Critical Reviews in Food Science and Nutrition, 58*(12), 1971–1985.
Marefati, A., Rayner, M., Timgren, A., Dejmek, P., & Sjöö, M. (2013). Freezing and freeze-drying of Pickering emulsions stabilized by starch granules. *Colloids and Surfaces A: Physicochemical and Engineering Aspects, 436*, 512–520.
McClements, D. J. (2012). Advances in fabrication of emulsions with enhanced functionality using structural design principles. *Current Opinion in Colloid & Interface Science, 17*(5), 235–245.
McClements, D. J., & Xiao, H. (2012). Potential biological fate of ingested nanoemulsions: Influence of particle characteristics. *Food & Function, 3*(3), 202–220.
Milsmann, J., Oehlke, K., Greiner, R., & Steffen-Heins, A. (2018). Fate of edible solid lipid nanoparticles (SLN) in surfactant stabilized o/w emulsions. Part 2: Release and partitioning behavior of lipophilic probes from SLN into different phases of o/w emulsions. *Colloids and Surfaces A: Physicochemical and Engineering Aspects, 558*, 623–631.
Milsmann, J., Oehlke, K., Schrader, K., Greiner, R., & Steffen-Heins, A. (2018). Fate of edible solid lipid nanoparticles (SLN) in surfactant stabilized o/w emulsions. Part 1: Interplay of SLN and oil droplets. *Colloids and Surfaces A: Physicochemical and Engineering Aspects, 558*, 615–622.
Paunov, V. N. (2003). Novel method for determining the three-phase contact angle of colloid particles adsorbed at air − water and oil − water interfaces. *Langmuir, 19*(19), 7970–7976.
Pawlik, A., Kurukji, D., Norton, I. T., & Spyropoulos, F. (2016). Food-grade Pickering emulsions stabilised with solid lipid particles. *Food & Function, 7*(6), 2712–2721.
Pichot, R., Spyropoulos, F., & Norton, I. T. (2009). Mixed-emulsifier stabilised emulsions: Investigation of the effect of monoolein and hydrophilic silica particle mixtures on the stability against coalescence. *Journal of Colloid and Interface Science, 329*(2), 284–291.
Salminen, H., Helgason, T., Aulbach, S., Kristinsson, B., Kristbergsson, K., & Weiss, J. (2014). Influence of co-surfactants on crystallization and stability of solid lipid nanoparticles. *Journal of Colloid and Interface Science, 426*, 256–263.
Schröder, A., Sprakel, J., Schroën, K., & Berton-Carabin, C. C. (2017). Tailored microstructure of colloidal lipid particles for Pickering emulsions with tunable properties. *Soft Matter, 13*(17), 3190–3198.
Schröder, A., Sprakel, J., Schroën, K., Spaen, J. N., & Berton-Carabin, C. C. (2018). Coalescence stability of Pickering emulsions produced with lipid particles: A microfluidic study. *Journal of Food Engineering, 234*, 63–72.
Sjöö, M., Emek, S. C., Hall, T., Rayner, M., & Wahlgren, M. (2015). Barrier properties of heat treated starch Pickering emulsions. *Journal of Colloid and Interface Science, 450*, 182–188.
Thompson, K. L., Williams, M., & Armes, S. P. (2015). Colloidosomes: Synthesis, properties and applications. *Journal of Colloid and Interface Science, 447*, 217–228.
Tzoumaki, M. V., Moschakis, T., Kiosseoglou, V., & Biliaderis, C. G. (2011). Oil-in-water emulsions stabilized by chitin nanocrystal particles. *Food Hydrocolloids, 25*(6), 1521–1529.
Wellen, B. A., Lach, E. A., & Allen, H. C. (2017). Surface pK_a of octanoic, nonanoic, and decanoic fatty acids at the air–water interface: Applications to atmospheric aerosol chemistry. *Physical Chemistry Chemical Physics, 19*(39), 26551–26558.
Zafeiri, I., Norton, J. E., Smith, P., Norton, I. T., & Spyropoulos, F. (2017). The role of surface active species in the fabrication and functionality of edible solid lipid particles. *Journal of Colloid and Interface Science, 500*, 228–240.
Zafeiri, I., Smith, P., Norton, I. T., & Spyropoulos, F. (2017). Fabrication, characterisation and stability of oil-in-water emulsions stabilised by solid lipid particles: The role of particle characteristics and emulsion microstructure upon Pickering functionality. *Food & function, 8*(7), 2583–2591.
Zhu, X.-F., Zhang, N., Lin, W.-F., & Tang, C.-H. (2017). Freeze-thaw stability of Pickering emulsions stabilized by soy and whey protein particles. *Food Hydrocolloids, 69*, 173–184.